

RESEARCH PAPER

Effect of Size and pH Variation on Antibacterial Activities of ZnS-ZnO Nanocomposite Towards Application in Water Treatment.

J. Barman

Department of Physics, ADP College, Nagaon, Assam, India

ARTICLE INFO

Article History:

Received 05 July 2021

Accepted 24 September 2021

Published 01 October 2021

Keywords:

Antimicrobial

Band gap

Nanocomposite

Photoluminescence

XRD

ABSTRACT

Stable and rapid zinc oxide and zinc sulphide nanocomposite with high antimicrobial efficiency was investigated by chemical route. The composite ZnS-ZnO has much importance because of their various application in different filed and as it shows enhanced and wide band gap with tunable size. The synthesized nanocomposite shows excellent antimicrobial activity in with sun light. The structural and size was estimated by various instrument like XRD, UV- Visible spectrometer, HRTEM, HRSEM and bonding was analyzed by FTIR analysis. Surface was studied through AFM. The sample in PL spectra shows the defect states and it was red shifted. The size of the particles were decreases when more photon induced in the samples. The size and band gap of the prepared samples depends mainly the parameters like ZnS and ZnO ratio, reaction time and pH of the composite. The optimizing ZnS-ZnO nanocomposite exhibits promising antibacterial effects in pathogens *Staphylococcus aureus*, *Bacillus subtilis*, *Klebsiella pneumoniae* and *Escherichia coli*. The energy band of nanocomposite is higher compared to individual bulk value of ZnS and ZnO. Due to the high chemical affinity and active antimicrobial activity, it has large possible application in water purification

How to cite this article

Barman J. Effect of Size and pH Variation on Antibacterial Activities of ZnS-ZnO Nanocomposite Towards Application in Water Treatment.. J Nanostruct, 2021; 11(4): 654-661. DOI: 10.22052/JNS.2021.04.003

INTRODUCTION

Nanotechnology has the great potential application because of tunable size and it can be manipulated in desired level. The smaller in size of semiconductor has shrinking effect and shows high chemical reactivity and good physical properties. When the confined dimension is less than de Broglie wavelength, quantum confinement occurs and shows unique optical properties that have led to opened the door for various application.

Among the various material the mix compound nanocomposite shows attractive properties in good conductivity and efficient antibacterial activities [1]. ZnO -ZnS are low toxic material and leading them to good interesting candidates for multiple applications in optoelectronic and biomedical

* Corresponding Author Email: jayantabarman2006@gmail.com

field. The ZnS-ZnO nanocomposite shows large surface to volume ratio and exhibits efficient antimicrobial activity. ZnO and ZnS semiconductor has direct and wide range band gap with mix phase. Both the shape has different structure and different bandgap energy making them exciting properties. The ZnS-ZnO nanocomposite shows in lower wave length optical absorption and red shift in photoluminescence (PL) properties [2].

Bacterial existence in drinking water becomes a major issue in developing countries. To remove the microbial agent though lots of effort has done yet composite semiconductor nanoparticles is the promising area for removal of microorganism because of high chemical affinity and photocatalytic activity [3].



This work is licensed under the Creative Commons Attribution 4.0 International License.

To view a copy of this license, visit <http://creativecommons.org/licenses/by/4.0/>.

The present work is mainly optimizing the synthesis technique with various parameter like reaction time, composite ratio, pH of the sample and photon induced time etc. The optimized sample were analyzed by various instrument like XRD, UV- Visible spectrometer, HRTEM, HRSEM, AFM and PL to investigate their structural, optical and morphological properties along with activity in microbial effect in human pathogens Staphylococcus aureus, Bacillus subtilis, Klebsiella pneumoniae and Escherichia coli.

MATERIALS AND METHODS

Materials

ZnO, ZnS, NaOH , ZnCl₂ and Na₂S were used from Merck, India. All the materials were used in high analytic grade. ZnCl₂ and ZnSO₄ was mixed at different concentration (1, 2, 3, 4 wt%) under a high stirring rate (250 rpm) condition. The constant temperature 70°C in 5 hours was maintained during the process of stirring. The sample under preparation was kept for 12 h for complete dissolution to get a transparent solution. To this solution, 2 wt% Na₂S was added until the complete solution turns into milky color and concentrated nitric acid to change the pH of the sample and zinc sulphate and sodium sulphide were added in different molar concentration ratio.

The samples were prepared in both powdered and thin film form and quantum dot formation is mainly responsible of Zinc ion exchanged reaction.

The growth of film is mostly considered the result of the surface aggregation of colloid particle (cluster- by -cluster growth) in the given experimental conditions. With change in pH the color changes from light milky to deep milky and optimum value for better adhesion in case of thin film form is 0.8 - 2. At the higher value of pH the size of nanoparticles increases due to the slow nucleation growth.

Preparation of antibacterial activity

Escherichia coli (MTCC 739), Staphylococcus aureus (MTCC-740), Klebsiella pneumonia (MTCC 432) and Pseudomonas aeruginosa (MTCC-424) were prepared for study of antibacterial efficacy in composite material. The microbial cultures were used from the "Microbial Gene Bank" (MTCC).

The bacteria were cultured at -4°C. Antibacterial process were done at optimized smallest particle at different pH value. The nutrient agar plates were applied for 3.0 ml of inoculums and swab

over the region. 6mm diameter were cut on the agar plates and the wells are placed with ZnO-ZnS nanoparticles. Standard antibiotic (Tetracyclin) was maintained for control the positive effect.

All samples were kept overnight at 37°C. The inhibition diameters were measured with sophisticated travelling microscope.

RESULTS AND DISCUSSION

UV-Vis Spectra analysis

The ZnO-ZnS nanocomposite prepared by chemical process in optimum conditions showed sharp absorbance beyond its band edge wave length 350 nm. Absorption spectra also show that the optimum pH value for larger blue shift and correspondingly for smaller dot.

It is observed that absorptions were shifted towards the shorter wavelength (or higher energy) region with decrease in pH. Moreover, the larger blue shift corresponding to smaller particle size indicated that strong confinement of nanocomposite. The photon induced time was also recorded and found that exposing time in sun light shows small size and effective microbial effect.

The energy band gap was calculated from Fig. 2. using a graph graph (αhν)² versus hν .From the graph band gap were calculated extrapolating the function straight-line to to (αhν)² = 0. From the shifting of band gap, radius of the particles is calculated using mass approximation model(EMA) [2].

$$E(R) = \frac{h^2 p^2}{2R^2} \left[\frac{1}{m_e^*} + \frac{1}{m_h^*} \right] - \frac{1.786e^2}{\epsilon R} - \frac{0.124e^4}{h^2 \epsilon^2} \left[\frac{1}{m_e^*} + \frac{1}{m_h^*} \right]^2$$

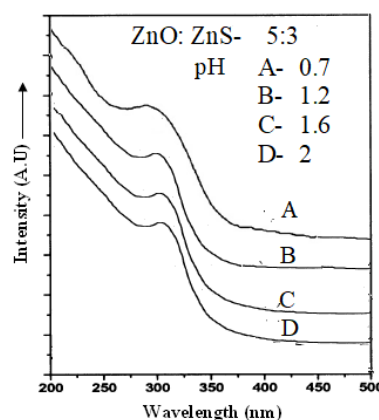


Fig. 1. UV Visible spectra at different pH of ZnO:ZnS-5:3 with of sun light at 5 hours



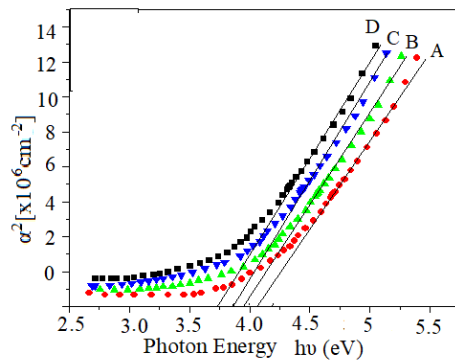


Fig. 2. Band gap composite ZnO-ZnS at different pH and composite ratio with sun light at 5 hours.

Table 1. Blue shift energy and particle size from optical model of ZnO-ZnS at different pH

Sample No.	ZnO:ZnS	pH	Band gap energy (eV)	Blue shift energy (eV)	Particle size from optical model (nm)
D	5:6	2	3.8	0.12	5.6
C	5:5	1.6	3.97	0.29	3.8
B	5:4	1.2	4.02	0.34	3.6
A	5:3	0.7	4.1	0.42	3

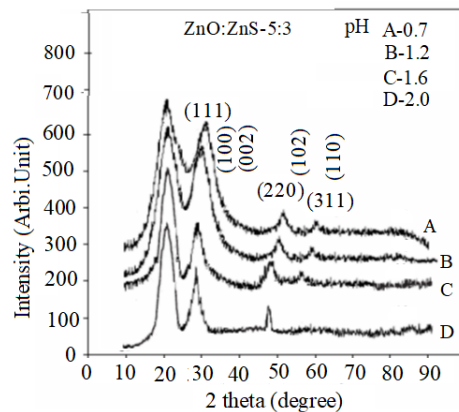


Fig. 3. XRD pattern composite ZnO-ZnS at 5:3 ratio and different pH with sun light at 5 hours.

where $E(R) = E_{np} - E_g$, E_g is the bandgap of the composite ZnO-ZnS nanoparticle, E_g the average band gap value of bulk ZnS and ZnO, m_e^* and m_h^* is the effective mass of electron and hole and r the radius of the particle. Using the above equation, particle size was estimated at different pH in optimum condition. The calculated particle size shows excitonic effect because it was less than de Broglie wave [4-5].

Table 1 Blue shift energy and particle size from optical model of ZnO-ZnS at different pH. Optical absorption and band gap estimation suggest that the composite material consist of single-phase cubic structure.

The shift of the absorption edge, which provides band gap energy, of the semiconductor to higher energy provides experimental evidence for such quantum confinement.

Structural Analysis by XRD

Fig. 3. shows four different spectra of ZnO-ZnS nanocomposite thin film form prepared at different pH of the solution ranging from 0.7 to 2.0. The XRD spectrum of A contain broad peaks at $2\theta = 29.370, 47.324$ indicating growth of nanostructure at pH =0.7. B also shows the peaks at $2\theta = 29.131, 47.164$, C at $2\theta = 28.942, 46.763$ and D at $2\theta = 28.752, 46.457$ for pH value 1.2, 1.6 and

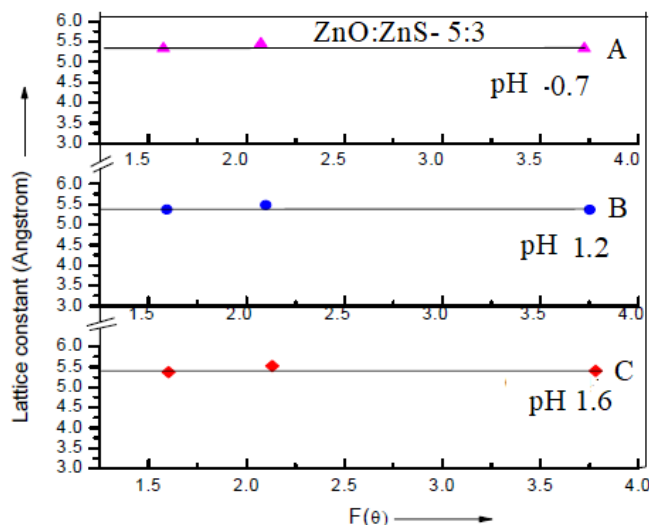


Fig.4. Nelson Relay plot of three samples ZnO-ZnS at 5:3 ratio and different pH in presence of sun light

2.0 respectively. The spectrum shows diffraction peaks corresponding to (111), (220) planes of Zinc blende(sphalerite) phase (JCPDS card, No. 5-0566) and (100),(002),(102),(110) for composite ZnO-ZnS. The XRD spectrum of all the spectra exhibit weak and broad peaks, suggesting small crystallite size. Again, it was observed that pH decreases more broadening take place with decreasing in crystallite size [4-6].

The increasing value of diffraction angle(2θ) suggest lattice contraction. The lattice contraction created decreasing crystallite size and increase in strain. The ratio of ZnO-ZnS maintained at 5:3 with expose in sun light. The effect of pH can be explained that in lower pH OH⁻ act as a catalyst for growing in composite nanoparticle. OH⁻ may increase the ionization strength of Zn²⁺ for faster reaction with S²⁻ and O²⁻ to accelerate the formation of nuclei. As formation of nuclei increases smaller particle coalescence and produce bigger particle [4].

Since we used a simple chemical process for composite thin film so possibility of twins formation can be neglected. Therefore, XRD peak broadening was considered only for size. The lattice parameter 'a' was determined with corresponding planes and systematic errors in 2θ were eliminated by Nelson and Riley plot in from three peaks. The corrected value of lattice constant "a" is calculated by F(θ) to zero. The lattice constant was explained in Fig. 4.

The average size of nanocrystal was determined using Scherer formula [2].

$$D = \frac{kl}{Vw_{2q} \cos q_B} \quad (2)$$

Where, q_B is the Bragg angle in radian and K=0.9 for spherical shape. The average crystalline was calculated 27 nm which is quite bigger than the size obtained in TEM and optical model.

FTIR Analysis

The interaction between ZnS and ZnO was analyzed by FTIR spectra. In Fig. 5. two characteristic bands at 3352 and 1092cm⁻¹ were observed. The band at 3352 cm⁻¹ in all spectra was due to O-H vibration band and another band at 1092 cm⁻¹ was due to hydroxy C-O stretching band. The OH⁻ group arises due to ZnO and ZnS nanoparticles. The band at 1700 cm⁻¹ probably appears due to water absorption while handling the sample in air [7].

The absorption peak at 2074 cm⁻¹ is the functional and can be assigned to -CH stretching mode of -CH₃ and -CH₂. The band 1638 cm⁻¹ agrees with C=O group. Weak band at 1018 cm⁻¹ can be form due to C-N vibrations of aliphatic amines. The main bands absorbed at 3443.95 cm⁻¹, 1638.18 cm⁻¹ and 669.97 cm⁻¹ indicates the existence of alcohols and phenols (O-H).

Antibacterial activity

The antibacterial activity was tested in four bacterial pathogenic bacteria E. coli, B. subtilis,

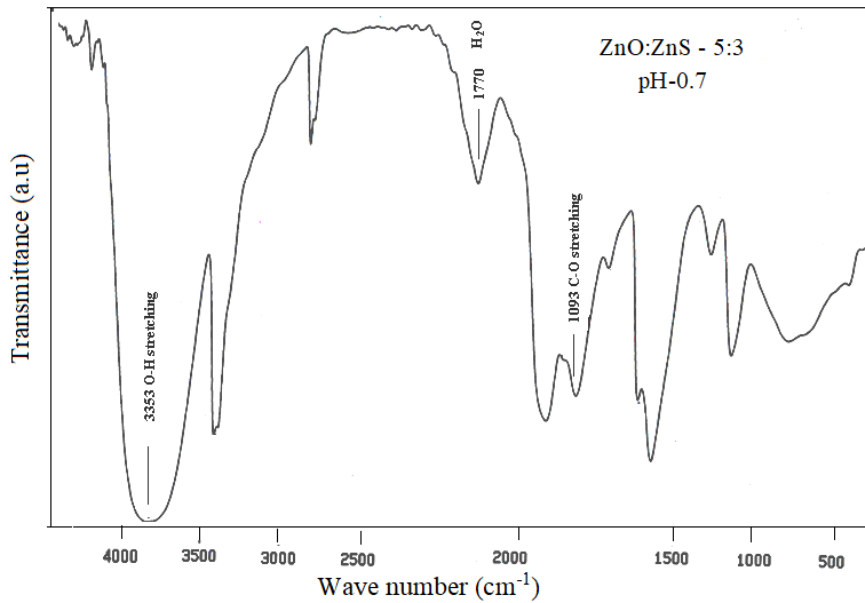


Fig. 5. FTIR spectrum of samples ZnO-ZnS at 5:3 ratio and at pH-0.7 with 5 hours sun light

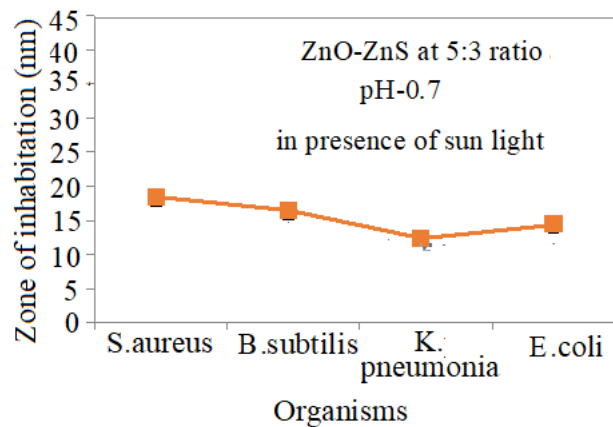


Fig. 6. Antibacterial activity of samples ZnO-ZnS at 5:3 ratio and at pH-0.7 with 5 hours sun light in four bacterial cultures

K. pneumoniae and S. aureus. Fig. 6 represents the zone of bacterial inhibition (diameter) 18mm, 16mm, 12mm and 14mm in E. coli, B. subtilis, K. pneumoniae and S. aureus bacterial suspension respectively. When the positive control, amoxicillin (1mg/ml) was tested for microbial activity against S. aureus, B. subtilis, K. pneumoniae and E. coli, the diameter of zone was 33mm, 35mm, 33mm and 38mm respectively [8-10].

Tetracyclin of 1mg/ml, concentration was perform control antibacterial agent. The results in Table-2 depict that Fe doped ZnO-ZnS nanoparticles are efficiently giving zone of inhibition. Table 2. Antibacterial efficacy of ZnO-ZnS nanopartecicles

with standard antibiotic in bacterial strains

PL Studies

For PL analysis the wavelengths were applied in between 250 nm to 400 nm. Fig. 7. Shows result of luminescence of ZnO-ZnS composite at 5:3 ratio and at different pH A-0.7, B-1.2 and C-1.6. All luminescence spectra clearly show that prepared samples have emission peak with high intensity at longer wave length. Another peak of smaller intensity is also observed at higher wave length

The peaks centered at 425 to 530 nm arises due to zinc and Sulphur vacancies in the lattice [11-15]. It is observed from the Fig.7 that peak

Table 2. Antibacterial efficacy of ZnO-ZnS nanoparteciles and standard antibiotic against four bacterial strains

Bacterial Strains	Zone of inhibition						Tetracycline (1mg.ml ⁻¹)
	ZnO-ZnS at 5:3 ratio and pH-0.7			ZnO-ZnS at 5:3 ratio and pH-0.7 in presence of sun light			
	50 µl	80 µl	100 µl	50 µl	80 µl	100 µl	100 µl
<i>E. coli</i>	5±0.15	9±0.12	17±0.14	5±0.15	10±0.12	19±0.12	34±0.09
<i>K. pneumoniae</i>	8±0.12	10±0.17	19±0.16	8±0.14	10±0.17	21±0.14	31±0.10
<i>B. subtilis</i>	2±0.16	9±0.15	16±0.12	3±0.16	8±0.16	16±0.12	30±0.1
<i>S. aureus</i>	5±0.12	11±0.09	19±0.12	5±0.12	12±0.14	21±0.14	33±0.12

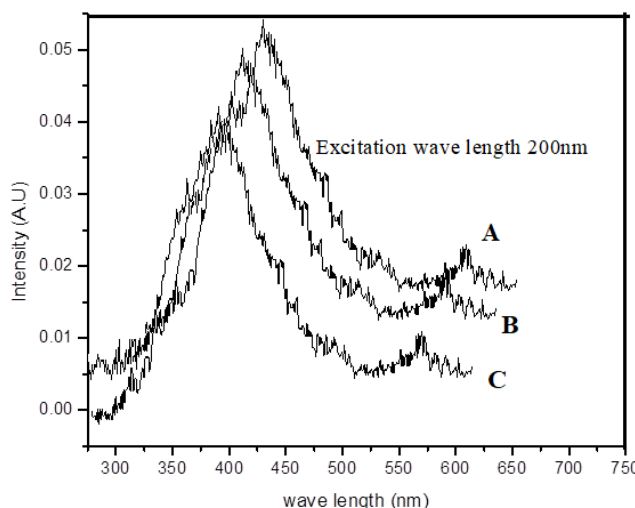


Fig.7. PL spectra ZnO-ZnS at 5:3 ratio and different pH in presence of sun light

Table 3. Stock shift energy of ZnO:ZnS-5:3 ratio at different pH

Sample	pH of composite material	Absorption peak (eV)	Emission peak (eV)	Stock shift energy (eV)	Size of the particle (nm) from TEM
A	0.7	4.15	2.61	1.54	4.1
B	1.2	3.99	2.63	1.36	4.7
C	1.6	3.92	2.67	1.24	6.85
D	2.0	3.86	2.72	1.14	7.89

position changes with the pH, which indicate the dependence on the particle size. The sample prepared at pH 0.7 showed greater emission intensity (at 425nm) then the sample prepared at other pH value. Thus, the pH takes an optimization factor for enhancement in PL. It is found that under the acidic condition, the Zn²⁺ and S²⁻ resides in a neighborhood of high OH⁻ ion and OH⁻ ions may take part in the lattice formation of ZnO-ZnS nanocomposite. The study reveals that pH takes an important parameter for improvement of emission intensity. Broad emission bands was due to the wide distribution of trap distance [16-20]. The stock shift energy was calculated from absorption and transmittance peak.

Table 2. represents stokes energy of a representative samples at different conditions. The large Stokes shift energy represents the strong

coupling to the lattice phonons. The strength of electron-phonon coupling with large particle size.

TEM, SEM and AFM studies

Fig.8. AFM direct image of ZnO-ZnS at 5:3 ratio and pH-0.7 in with sun light our optimum antimicrobial effect. The TEM image shows that the size of the particle was spherical in shape and found in the range 5-8nm which was a good similarity as size obtained in optical model. Fig. 9 represent the SEM photograph of ZnO:ZnS nanocomposite at optimum size and antimicrobial effect. It was found that some grains are overlap and showed different shape. The SEM photo images were not very sharp because of lower operating voltage (15KV). The images were observed at lower operating voltage to avoid sample damage. Higher operating voltage could have improved the



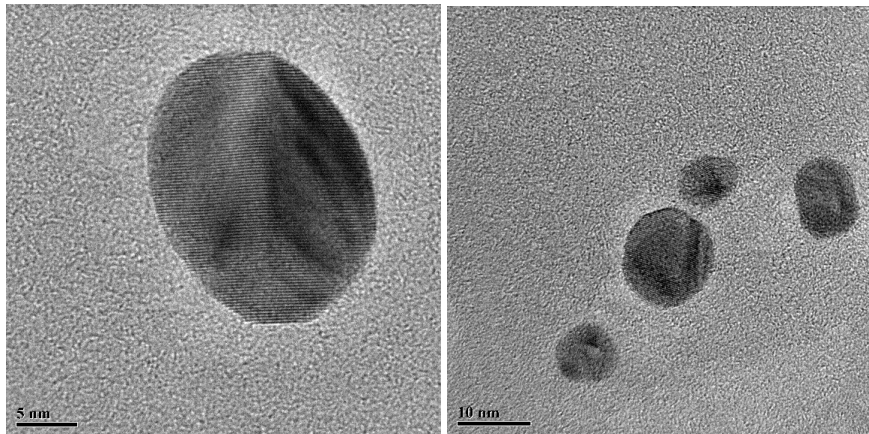


Fig. 8. HR TEM image of ZnO:ZnS-5:3

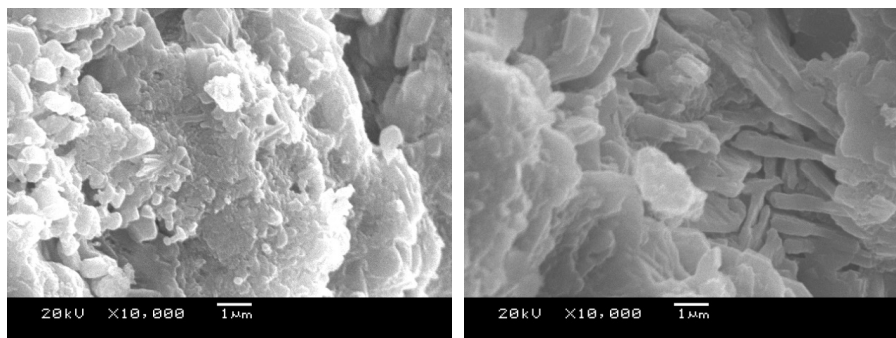


Fig. 9. HR-SEM Micrograph of ZnO:ZnS-5:3

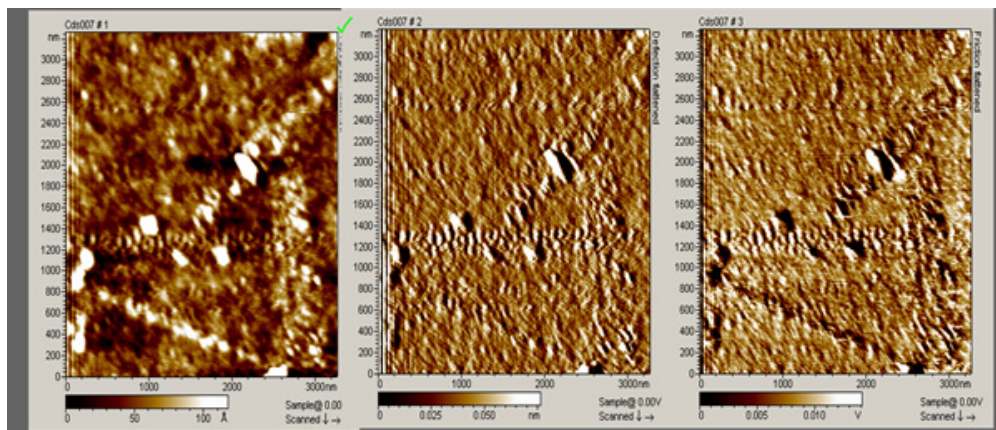


Fig. 10. AFM image of ZnO:ZnS-5:3 at pH 2.0,1.2 and 0.7

image sharpness and resolution [20-25]. Fig.10 showed the AFM (contact mode) images of the ZnO-ZnS nanocomposite at different pH ranging.

Images showed that with decreasing pH the sharp smoothness takes place i.e roughness decreases. The Fig represent the ZnO:ZnS-5:3 at pH 2.0,1.2 and 0.7 from left to right and observed that at lower pH pyramid shape becomes clear and

it is evidence of Zinc blende (Sphalerite) structure.

CONCLUSION

ZnO-ZnS nanocomposite in optimum condition has been establish for better efficient in antimicrobial activity. Again, small and spherical dot exhibit better antimicrobial effect. The size was confirmed by XRD, TEM, optical model and

SEM. Antimicrobial effect was calculated with the important pathogens *Staphylococcus aureus*, *Bacillus subtilis*, *Klebsiella pneumoniae* and *Escherichia coli*. UV Visible and PL properties shows the pH takes a major role for formation of small particle and desired band gap. PL analysis showed the emission were red shifted and optical study showed that absorption was blue shifted. The lattice parameter was confirmed by Nelson Relay plot with XRD. AFM image represents the surface topography with change of pH.

ACKNOWLEDGEMENTS

I would like to acknowledge Department of Biotechnology (DBT), Ministry of Science & Technology, Government of India for financial assistance through star college and Biotech HUB scheme. We would also like to acknowledge ASTEC for financial support. We would like to acknowledge Department of Molecular Biology and Biotechnology, Tezpur University for providing FTIR facilities.

CONFLICT OF INTEREST

The authors declare that there is no conflict of interests regarding the publication of this manuscript.

REFERENCES

- Desselberger U. Emerging and re-emerging infectious diseases. *J. Infect.* 2000;40:3–15.
- Barman J, Sultana F. Opto electronics and antimicrobial activity of composite Zinc Sulphide and Cadmium sulphide Quantum dot and application in water treatment. *Indian Journal of Pure and Applied Physics.* 2017; 55: 231-136.
- Ramyajuliet Madhavan, Priyanka Beulah Gnana raj Gnana, Tresin Pious Soris, Doss Asirvatham, Mohan Veerabahu Ramasamy. Biogenic synthesis of copper nanoparticles using aquatic pteridophyte *Marsilea quadrifolia* Linn. rhizome and its antibacterial activity. *Int. J. Nano Dimens.* 2020; 11 (4): 337-345.
- Ali Salman, Saleem Sumaiya, Salman Muhammad, Khan Majid. Synthesis, structural and optical properties of ZnS–ZnO nanocomposites. *Materials Chemistry and Physics.* 2020; 248 :122900
- Nelson J.B., Riley D.P. *Proc. phys. Soc. (London).* 1945; 57:160.
- Retchkiman-Schabes P.S., Canizal G, Becerra-Herrera R, Zorrilla C, Liu H.B., Ascencio J.A. Biosynthesis and characterization of Ti/Ni bimetallic nanoparticles. *Opt. Mater.* 2006;29: 95–99.
- Gu H, Ho PL, Tong E, Wang L, Xu B. Presenting vancomycin on nanoparticles to enhance antimicrobial activities. *Nano Lett.* 2003;3 :1261–1263.
- Prabhu S, Poulouse E.K. Silver nanoparticles: mechanism of antimicrobial action, synthesis, medical applications and toxicity effects. *Int. Nano Lett.* 2012;5:32–42.
- Bora J.P., Barman J., Sarma K.C. Structural and optical properties of CdS nanoparticles. *Chalcogenide Letters.* 2008; 5(9): 201.
- K.K.Nanda, S.N.Sarangi, S.N.Sahu. CdS Nanocrystalline films: Composition, surface, crystalline size, structural and optical absorption studies. *Nano Structured Materials.* 1998;10:1401.
- M. Sookhikian, Y.M. Amin, W.J. Basirun, M.T. Tajabadi, N. Kamarulzaman. Synthesis, structural, and optical properties of type-II ZnO-ZnS core-shell nanostructure. *J. Lumin.* 2014;145: 244–252.
- S. Baruah, J. Dutta. Growth of ZnO nanostructures, *Sci. Technol. Adv. Mater.* 2009; 10: 208.
- W. Chen, Z. Wang, Z. Lin, L. Lin, (1997), Thermoluminescence of ZnS Nanoparticles. *Appl. Phys. Lett.* 20 :1465–1467
- Barman J, Sarma K.C. Effect of pH on ZnS nanocrystalline thin film embedded in a polyvinyl alcohol matrix. *International Journal of modern physics B.* 2010;24(29): 5663–5673.
- Barman J, Bora J.P., Sarma K.C. Synthesis and characterization of CdS nanoparticles by chemical growth technique. *Journal of Optoelectronics and Advanced Material - Rapid Communication.* 2008;2(12) :770
- Parida P., Behera A., Swain S.K., Mishra S.C. Characterization of nanoparticles through SEM, FTIR, XRD & DSC. *Fitoterapia.* 2011;3: 253-269.
- Perez C., Paul M, Bazeraue P. Antibiotic assay by agar well diffusion method. *Acta Biol Med Exp.* 1990;15:113-115.
- Shankar S.S., Ahmad A, Pasricha R, Sastry M. Bioreduction of chloroaurate ions by geranium leaves and its endophytic fungus yields gold nanoparticles of different shapes. *J. Mater. Chem* 2003;13:1822–1826.
- D.K. Mondala, C. Borgohainb, N. Paula, J.P. Boraha. Tuning hyperthermia efficiency of MnFe₂O₄/nS nanocomposites by controlled ZnS concentration. 2016 <https://doi.org/10.1016/j.jmrt.2019.09.034>
- Tao Gengi, Shuangbin Zhang, Yao Chen. Study on the synthesis and photocatalysis of Ag₃PO₄ polyhedral Microcrystals *Bull Mater Sci.* 2020;43:223
- Tude S. C., Zubku M., Kusz J., Bhattacharjee A. Structural, morphological and optional characterization of green synthesized ZnS nanoparticles using *Azadirachta indica* (Neem) leaf extract. *Int. J. Nano Dimens.* 2020; 11: 99-111.
- Tran F., Blaha P. Accurate band gaps of semiconductors and insulators with a semilocal exchange correlation potential. *Phys. Rev. Lett.* 2009; 102: 226401-226405
- Lam S. M., Sin J. C., Abdullah A. Z., Mohamed A. R. Degradation of wastewaters containing organic dyes photocatalysed by zinc oxide: A review. *Desalination. Water Treatment.* 2012;41: 131-169
- Guo H., Chen J., Weng W., Wang Q., Li S. Facile template-free one-pot fabrication of ZnCo₂O₄ microspheres with enhanced photocatalytic activities under visible-light illumination. *Chem. Eng. J.* 2014; 239: 192-199
- Sinthiya M. M. A., Ramamurthi K., Mathuri S., Manimozhi T., Kumaresan N., Margoni M. M., Karthika P. C. Synthesis of Zinc Ferrite (ZnFe₂O₄) nanoparticles with different capping agents. *Int. J. Chem. Tech. Res.* 2015;7: 2144- 2149.